

Communication

Zinc Oxide Tetrapods Doped with Silver Nanoparticles as a Promising Substrate for the Detection of Biomolecules via Surface-Enhanced Raman Spectroscopy

Edgars Vanags ^{*}, Ivita Bite, Liga Ignatane, Reinis Ignatans, Annamarija Trausa , Ciro Federiko Tipaldi, Karlis Vilks  and Krisjanis Smits

Institute of Solid State Physics, University of Latvia, 8 Kengaraga st., LV1063 Riga, Latvia

* Correspondence: edgars.vanags@cfi.lu.lv

Abstract: In this study, we report the fabrication and characterization of silver nanoparticle-doped zinc oxide tetrapod substrates used for surface-enhanced Raman scattering to detect rhodamine B. Prior to this, silver nanoparticle-doped zinc oxide tetrapods were synthesized using the solar physical vapor deposition method. Subsequently, silver-doped zinc oxide tetrapods were applied onto silicon wafers via the droplet evaporation process. The surface-enhanced Raman scattering activity of the silver nanoparticle-doped zinc oxide tetrapod substrate was evaluated by detecting rhodamine B using Raman spectroscopy. Our results demonstrate that the silver nanoparticle-doped zinc oxide tetrapod substrate exhibits surface-enhanced Raman scattering activity and can detect rhodamine B at concentrations as low as 3 $\mu\text{g}/\text{mL}$. This study suggests that silver nanoparticle-doped zinc oxide tetrapod substrates have potential as surface-enhanced Raman scattering platforms as well as potential for the detection of biomolecules.

Keywords: ZnO; tetrapods; silver nanoparticles; SERS; rhodamine B detection



Citation: Vanags, E.; Bite, I.; Ignatane, L.; Ignatans, R.; Trausa, A.; Tipaldi, C.F.; Vilks, K.; Smits, K. Zinc Oxide Tetrapods Doped with Silver Nanoparticles as a Promising Substrate for the Detection of Biomolecules via Surface-Enhanced Raman Spectroscopy. *ChemEngineering* **2024**, *8*, 19. <https://doi.org/10.3390/chemengineering8010019>

Academic Editors: Alirio E. Rodrigues and Rajinder Pal

Received: 17 November 2023

Revised: 27 December 2023

Accepted: 30 January 2024

Published: 4 February 2024



Copyright: © 2024 by the authors. Licensee MDPI, Basel, Switzerland. This article is an open access article distributed under the terms and conditions of the Creative Commons Attribution (CC BY) license (<https://creativecommons.org/licenses/by/4.0/>).

1. Introduction

Various measurement and diagnostic methods are currently employed in the fields of biology and medicine. However, the recent global pandemic and associated lockdowns have underscored the persistent need for more accurate, time-efficient, and cost-effective analytical techniques, particularly when dealing with biomedical samples [1–3].

The conventional approach of collecting a biological sample and sending it to a laboratory, where it may take hours or days to obtain the results during a pandemic outbreak, is incapable of providing timely and rapid diagnostic information. There is an urgent requirement for an easy-to-use device that allows for on-site instant testing [4–7]. For such requirements, surface-enhanced Raman scattering (SERS) represents the potential for an easy-to-use device that enables on-site testing technology with high sensitivity and selectivity [4,8,9]. However, there are presently no readily available point-of-care testing solutions based on this approach [4,5]. This is primarily due to the complexity of measurement systems, the reproducibility issues of SERS substrates, and the high fabrication costs of SERS substrates. In the case of complex Raman spectra, particularly in metals where additional peaks frequently emerge, the interpretation of such spectra can be even more challenging and could require the assistance of computational Raman spectra obtained through first principle calculations to aid in deciphering these complex spectra [10,11].

The analytical method SERS is based on the idea of Raman scattering, which is a phenomenon in which a molecule scatters light, changing the wavelength of the light [12]. In addition to Raman, the scattering effect is amplified by electromagnetic and/or chemical enhancement [13]. In SERS, the Raman scattering signal is enhanced by many orders of magnitude, making it possible to detect even extremely small amounts of molecules [14].

Many advantages of SERS are attributed to its substrate; therefore, the choice of the substrate significantly impacts the performance of SERS and the quality of the obtained signal [15]. To understand the influence of substrate choice on SERS performance, it is essential to delve into the fundamental process of signal enhancement.

In SERS, Raman scattering is electromagnetically amplified due to the increased interaction of light with metal particles, typically composed of silver or gold [16], which mutually interact with molecules. This electromagnetic enhancement is due to the collective oscillations of electrons on the surface of the metal, known as surface plasmon resonances, which lead to increased interaction between the analyte molecules and the metal surface [17].

In addition to electromagnetic enhancement, another crucial mechanism in SERS is chemical enhancement [18]. Chemical enhancement involves charge transfer and resonance interactions between the analyte molecules and the metal nanoparticle surface [19]. This phenomenon can significantly boost Raman scattering signals beyond that which electromagnetic enhancement alone achieves.

Chemical enhancement occurs when the analyte molecules chemisorb onto the metal surface, allowing for strong chemical interactions [14]. This interaction can lead to alterations in the molecular structure of the analyte, enhancing its Raman scattering activity. Furthermore, resonance effects can occur when the excitation laser coincides with the electronic transitions of the analyte, amplifying the Raman signal [20].

A variety of substrates, including metals [21,22], metal oxides [23], carbon materials [24], and polymers [25], can be used for SERS, and each has its own advantages and disadvantages. The choice of the substrate depends on the specific requirements of the SERS analysis, including the type of sample being analyzed, the desired SERS enhancement, and the cost of the substrate.

While various substrates have been employed for SERS [26–29], silver nanoparticles have gained popularity due to their remarkable optical and physical properties [30–32]. These nanoparticles exhibit strong surface plasmon resonances [33], significantly amplifying the Raman scattering signal. However, our approach to Raman enhancement goes beyond the conventional strategies that rely solely on electromagnetic and chemical effects.

In this study, we took an approach that involved applying the three-dimensional (3D) displacement of substrate nanoparticles, which augments Raman enhancement in multiple aspects [34]. The 3D displacement not only results in an expanded surface area but also provides more attachment sites for analyte molecules [35]. This larger active surface area promotes a higher interaction between the target molecules and the metal nanoparticles, further enhancing the Raman signal. Moreover, the 3D arrangement increases the interference and allows for Raman signal enhancement in multiple directions, creating an SERS-effective substrate [36].

For this purpose, we chose ZnO tetrapods due to their advantageous properties [37] as a cost-effective matrix for silver nanoparticle deposition. This result is achieved through the solar physical vapor deposition method, where both ZnO tetrapods and silver nanoparticles are deposited in one-step synthesis.

From our expectations, integrating silver nanoparticles onto ZnO tetrapods offers several advantages for Raman enhancement. Firstly, ZnO tetrapods provide a high surface area, which can facilitate the adsorption of target molecules and enhance their interaction with the metal nanoparticles. The unique morphology of ZnO tetrapods, with their extended branches and sharp tips, provides numerous attachment sites for the metal nanoparticles, allowing for the high density of active sites for Raman scattering.

Furthermore, the integration of silver nanoparticles onto ZnO tetrapods can create a synergistic effect. The combination of the plasmonic properties of the metal nanoparticles and the semiconducting properties of ZnO could lead to a dual enhancement mechanism. The metal nanoparticles can enhance the local electromagnetic field around the tetrapods, leading to an increased Raman signal through the electromagnetic enhancement mechanism. Additionally, the charge transfer between the metal nanoparticles and the ZnO tetrapods

can enhance the charge distribution and improve the charge-transfer resonance, resulting in enhanced Raman scattering through the chemical enhancement mechanism. The scheme of SERS achieved using our proposed substrate is depicted in Figure 1.

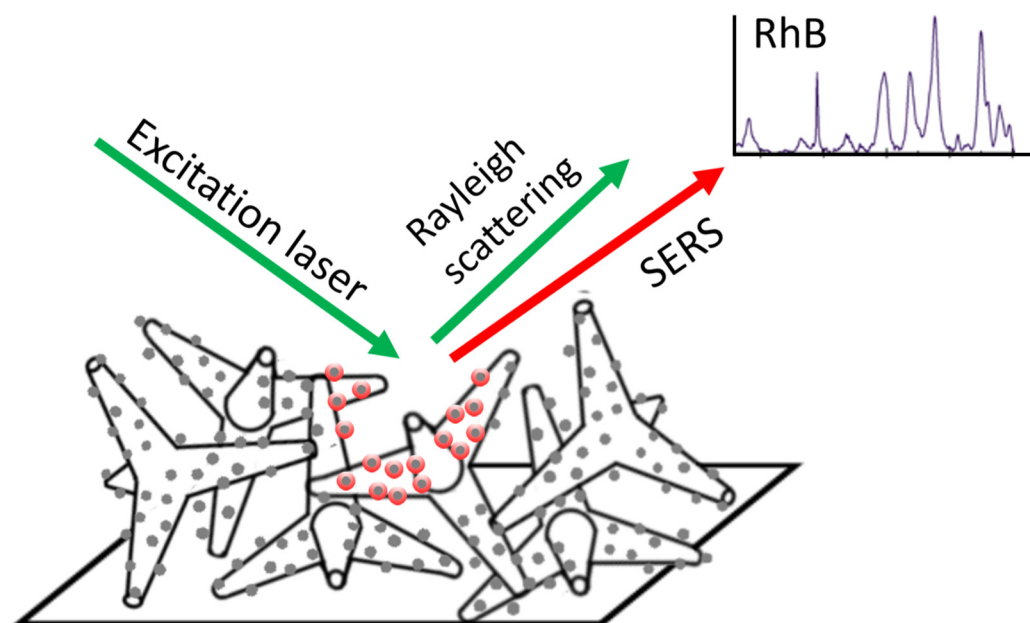


Figure 1. An illustration of the designed SERS substrate is depicted, featuring a silicon base on which multiple layers of silver nanoparticle-doped zinc oxide (ZnO-Ag) tetrapods are displaced, and the substrate is excited by a laser, including the formation of Raman signal-enhancing “hotspots” (represented as the red shells) in proximity to the silver nanoparticles (represented as the grey dots).

In addressing the challenges inherent in the diagnosis of biological samples, our research investigates the potential of ZnO-Ag tetrapods as SERS substrates for biomolecule detection. While the primary focus is on the ultimate application of our substrates in the sensitive detection of diverse biomolecular species, we initially conducted investigations using Rhodamine B (RhB) as a model analyte. This intentional choice provides a more controlled and reproducible environment to elucidate the efficacy of developed SERS substrates, offering valuable insights into the fundamental interactions between the developed SERS substrates and analytes. The use of RhB in the early investigations serves as a stepping stone, guiding the development of SERS substrates toward broader applications in biomedical diagnostics.

2. Materials and Methods

2.1. Synthesis

ZnO-Ag tetrapods were synthesized using solar physical vapor deposition with the following two distinct targets: pressed zinc dust/metallic silver nanoparticles and pressed silver ion-containing zinc xerogel (ZnX). The atomic percentage of silver in the targets was varied, though it was specifically set at 0 at.% (Ag0), 1 at.% (Ag1), 5 at.% (Ag5), and 10 at.% (Ag10). In total, eight different tetrapods were obtained through these two synthesis approaches. A comprehensive description of the methodology is provided in our forthcoming study.

2.2. Characterization of ZnO-Ag Tetrapods

Scanning transmission electron microscopy (STEM) measurements for single ZnO-Ag tetrapods were performed using a Thermo Fisher (Eindhoven, The Netherlands) Scientific SEM Helios 5 UX apparatus equipped with a high-angle annular dark-field (HAADF) detector. A suspension of ZnO-Ag tetrapods in ethanol was applied onto holey carbon films on 400 mesh copper grids and left at room temperature to dry. The tetrapods were

then analyzed via imaging under a microscope in the STEM mode operating at 30 kV voltage and a 50 pA current. The HAADF detector was used to obtain images of the tetrapods, and the images were processed using ImageJ software (version 2.9.0/1.53 t) [38] to determine the size and shape of the tetrapods.

To prepare the synthesized Ag-doped ZnO tetrapods for energy-dispersive X-ray spectroscopy (EDX) measurements, a small amount of the powder was pressed into indium using a hydraulic press. The pressure applied during the pressing was carefully controlled to ensure that the sample was compact and uniform in thickness. Indium was used as a backing material for the sample to prevent any charging effects during the measurement. The use of indium also provided a good surface for the sample to adhere to, which ensured that the sample was stable during the measurement. The sample was then placed on the sample holder for analysis. EDX measurements were carried out to determine the elemental composition of Ag-doped ZnO tetrapods. The measurements were performed using a Thermo Fisher Scientific SEM Helios 5 UX apparatus equipped with an EDX detector. The EDX spectra were collected by focusing a beam of electrons onto the sample surface and detecting the characteristic X-rays emitted by the atoms in the sample operating at a 20 kV voltage. The spectra were analyzed to determine the atomic composition of the tetrapods and to confirm the presence of silver in the samples. The EDX measurements were performed at least in triplicate to ensure the reproducibility of the results. The data obtained from the EDX analysis were processed using Thermo Scientific™ Pathfinder™ software (version 2.8) to obtain the elemental composition and concentration of the silver in ZnO tetrapods.

X-ray diffraction (XRD) was employed to investigate the crystallographic structure of the synthesized ZnO-Ag tetrapods. The XRD measurements were performed using a Malvern PANalytical (Almelo, The Netherlands), XPert PRO instrument at room temperature. Prior to XRD analysis, a small amount of the synthesized tetrapods was placed onto a glass slide and spread evenly to form a thin layer. XRD analysis was carried out using Cu K α radiation ($\lambda = 0.154$ nm).

2.3. Fabrication of SERS Substrates

To fabricate the SERS substrates, ZnO-Ag tetrapods (0.0050 g) were dispersed in ethanol (1 mL) by shaking the samples on an orbital shaker for 30 min each. Subsequently, the suspensions were applied using the droplet evaporation method to the (100)-oriented Si wafers of two-side-polished MicroChemicals Silicon p-type (Boron) substrates, cut into 5×5 mm with thicknesses of 500 ± 15 μ m.

Initially, a 3 μ L droplet of the prepared solution was dispensed onto a clean silicon substrate with a micropipette. The droplet was allowed to evaporate on a heating plate at 40 °C. The droplet–evaporation process was repeated nine times for each substrate. During the evaporation process, the nanoparticles concentrated at the edges of the droplet, forming self-assembled multilayers of nanoparticles.

2.4. Characterization of SERS Substrates by SEM

To analyze the morphology and overall quality of the ZnO tetrapods layer, the obtained substrates were characterized using a Thermo Fisher Scientific SEM Helios 5 UX apparatus. The samples of SERS substrates were mounted with carbon tape on aluminum stubs. Scanning electron microscopy (SEM) analysis was conducted at an acceleration voltage of 2 kV and a current of 25 pA. SEM images were captured at various magnifications to study the surface features and the distribution of ZnO tetrapods.

2.5. Preparation of RhB Solution Series

To prepare a RhB solution in isopropanol, RhB (Dye content $\geq 90\%$) and isopropanol (ACS reagent, $\geq 99.5\%$) were purchased from Sigma-Aldrich (Darmstadt, Germany). Then, a 6.1×10^{-5} M RhB solution in isopropanol was prepared by dissolving RhB in isopropanol to achieve the desired concentration. Subsequently, this initial solution was subjected to

dilution steps to obtain five additional solutions with concentrations of 6.1×10^{-6} M, 6.1×10^{-7} M, 6.1×10^{-8} M, 6.1×10^{-9} M, and 6.1×10^{-10} M. The dilutions were carried out systematically to create a range of RhB concentrations for experimental purposes.

2.6. Raman Measurements

For Raman measurements, a series of RhB solutions in ethanol of varying concentrations ranging from 6.1×10^{-5} to 6.1×10^{-10} mol/L were used. An aliquot (3 μ L) of each solution was deposited onto the SERS substrate and allowed to dry at room temperature. The SERS activity of ZnO tetrapod substrates was measured using a Raman spectrometer TriVista CRS Confocal Raman Microscope (TR777), Spectroscopy & Imaging GmbH (Warstein, Germany). The SERS measurements were performed at room temperature using a laser excitation wavelength of 532 nm. The Raman spectra were acquired with an integration time of 1 s, and the laser power was kept constant (~462 mW) throughout the measurements to minimize any thermal effects. The SERS spectra were analyzed using OriginPro 2021 software.

3. Results

3.1. Morphological Studies

All eight obtained samples of ZnO-Ag tetrapods with varying silver content were analyzed using STEM. Our observations revealed that the morphology of the ZnO-Ag tetrapods changed with the increasing silver content in both scenarios, whether synthesized from the metallic target or the xerogel target. As the silver content increased, we observed an increase in tetrapod shape defects, indicating a less ideal tetrapod structure. Furthermore, the tetrapods synthesized from the zinc xerogel target exhibited a higher presence of structural defects compared to those synthesized from metallic zinc dust. Additionally, we observed an increased tetrapod agglomeration with higher silver content. In HAADF images, the deposition of silver nanoparticles onto the tetrapod surface was clearly visible, as the silver nanoparticles appeared brighter. The presence of silver nanoparticles on the tetrapod surface became evident even in samples synthesized with 1% silver-containing targets. The obtained STEM images of ZnO-Ag tetrapod samples are depicted in Figures 2 and 3.

Furthermore, we aimed to evaluate the potential of ZnO-Ag tetrapods with varying silver content as SERS substrates. To investigate their SERS performance, we employed the droplet evaporation process for substrate preparation. This process allowed us to apply the ZnO-Ag tetrapods on silicon wafers, creating a relatively uniform and organized substrate surface. The surface of the obtained substrates was evaluated using SEM. The acquired images are depicted in Figures 4 and 5.

3.2. Elemental Composition Analysis: Insights from EDX Measurements

In the EDX analysis, the elemental composition of eight distinct samples, comprising four tetrapod samples derived from silver ions containing zinc xerogel targets and another four samples obtained from metallic zinc dust and silver nanoparticles, was determined in terms of their atomic percentage. As shown in Table 1, the elements analyzed included zinc, oxygen, and silver. The results reveal a near 1:1 stoichiometry between zinc and oxygen for all the samples, aligning with the expected composition within the safety intervals of the measurement technique. The EDX data show that there was significantly more silver in tetrapod samples made from zinc xerogel compared to those made from metallic zinc and silver targets. This suggests that achieving the more efficient decoration of ZnO tetrapods with silver nanoparticles is possible when utilizing silver ions in zinc xerogel, in contrast to employing metallic zinc dust and silver nanoparticles.

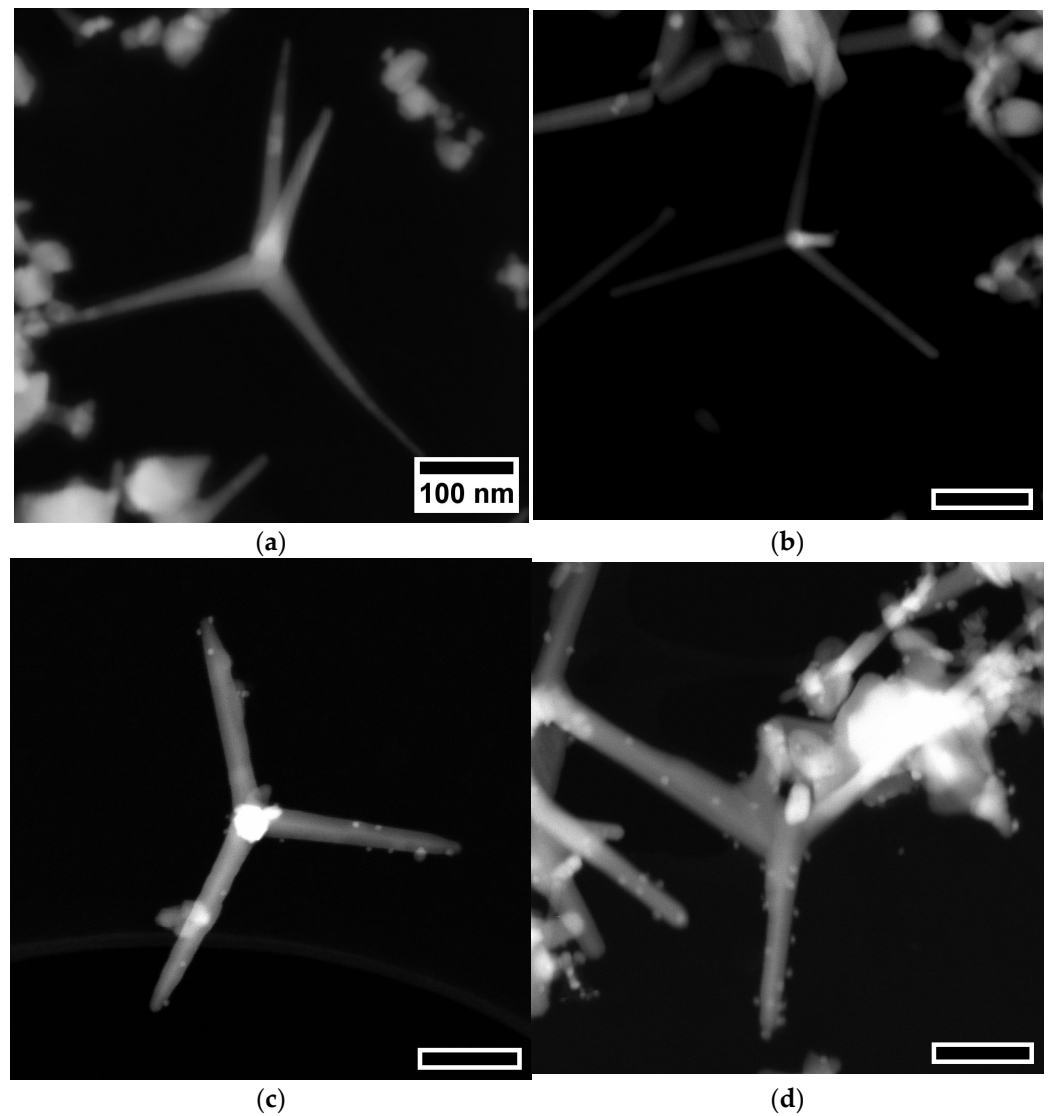


Figure 2. STEM images obtained in the HAADF mode of ZnO-Ag tetrapods synthesized from metallic zinc dust and silver nanoparticle targets with varying silver content: (a) 0 a%; (b) 1 a%; (c) 5 a%; (d) 10 a%.

Table 1. Elemental composition of ZnO tetrapods decorated with silver nanoparticles synthesized from different targets.

Sample	Zinc, Atomic %	Oxygen, Atomic %	Silver, Atomic %
ZnAg0	51.1 ± 7.5	48.9 ± 7.8	-
ZnAg1	51.1 ± 6.0	48.7 ± 6.0	0.15 ± 0.12
ZnAg5	51.7 ± 2.4	46.7 ± 1.7	1.5 ± 1.4
ZnAg10	49.5 ± 5.3	48.7 ± 0.2	4.1 ± 1.9
ZnXAg0	52.5 ± 1.5	47.5 ± 1.2	-
ZnXAg1	46.5 ± 4.3	50.4 ± 2.7	3.4 ± 2.9
ZnXAg5	46.5 ± 6.4	47.6 ± 4.7	5.9 ± 1.1
ZnXAg10	38.3 ± 2.0	44.5 ± 2.6	17.3 ± 0.9

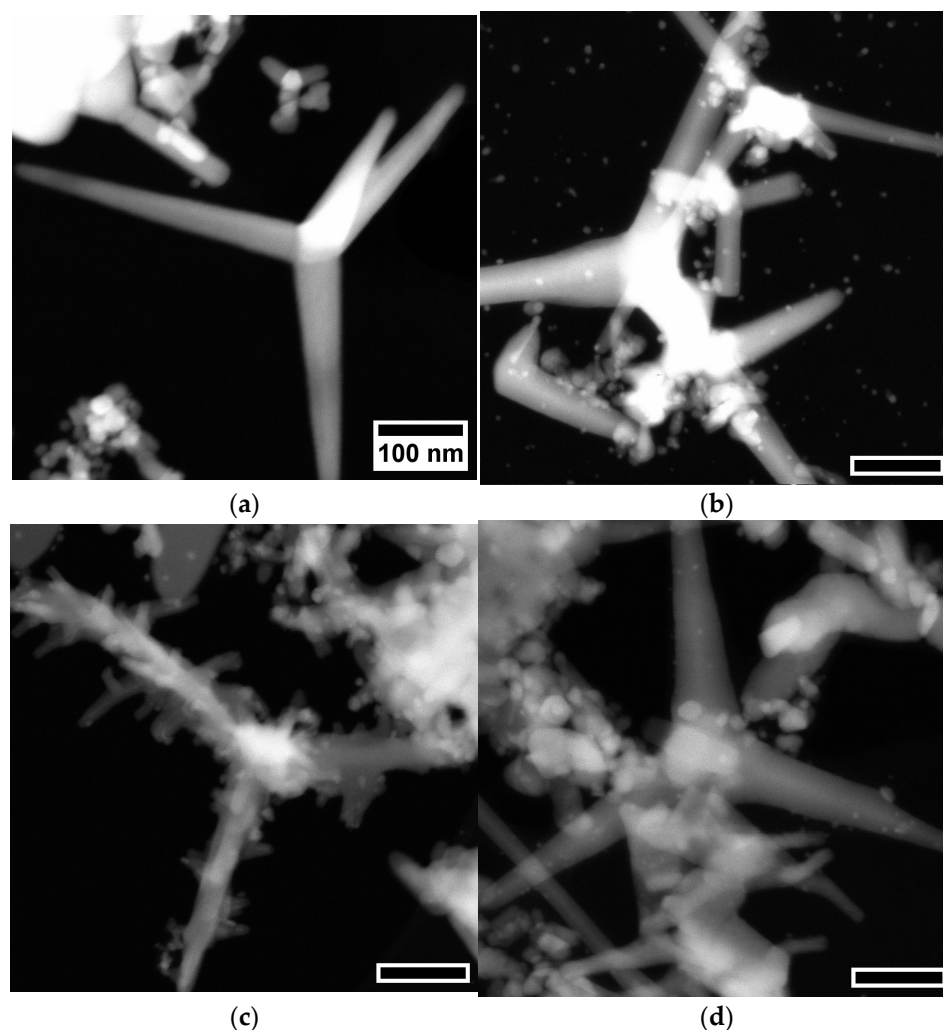


Figure 3. STEM images obtained in the HAADF mode of ZnO-Ag tetrapods synthesized from silver ion-containing zinc xerogel targets with varying silver content: (a) 0 a%; (b) 1 a%; (c) 5 a%; (d) 10 a%.

3.3. XRD Analysis

The XRD patterns for all eight synthesized ZnO-Ag tetrapods were analyzed, and diffraction pattern comparisons were made using the Match! software (version 3.14) PDF-4+ database. The obtained results provided the crystallographic structures of the synthesized tetrapods, as depicted in Figure 6. The diffraction patterns revealed distinct peaks corresponding to cubic Ag and hexagonal ZnO phases. The presence of these characteristic peaks indicates the successful incorporation of silver nanoparticles into the ZnO tetrapod structures. The peaks associated with cubic Ag were identified at the same angles as those provided in the database, and their intensities were examined. The relative intensity of these peaks was found to correlate with the Ag content in the samples, as determined using EDX measurements. Specifically, the diffraction patterns demonstrated the highest intensity of cubic Ag peaks in the case of the ZnO tetrapods synthesized from silver ion-containing zinc xerogel, especially for the ZnXAg10 sample, aligning with the EDX data, which revealed the highest concentration of silver in this sample.

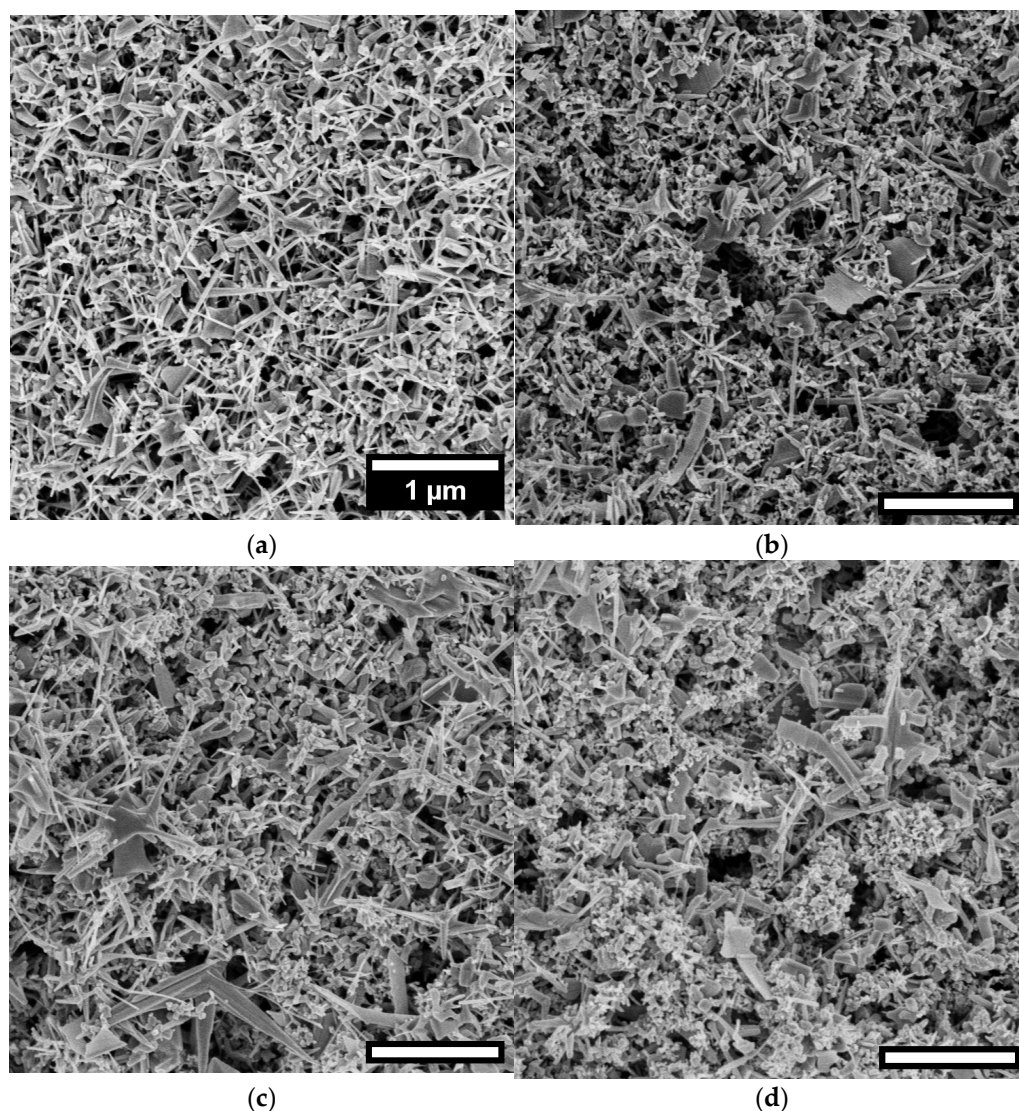


Figure 4. SEM images of ZnO-Ag tetrapod substrates synthesized from metallic zinc dust and silver nanoparticle targets with varying silver content: (a) 0 a%; (b) 1 a%; (c) 5 a%; (d) 10 a%.

3.4. SERS Studies

Subsequently, we applied RhB, a common Raman-active molecule, to the prepared substrates. The prepared SERS substrates were subjected to Raman spectroscopy to examine their ability to enhance the Raman signals of RhB. The Raman spectra were analyzed to discern any notable differences in signal enhancement among the eight different tetrapod samples with varying silver content.

Our results show distinct variations in SERS signal enhancement among the different samples, depending on the silver content and synthesis method. The spectra obtained from these substrates reveal that SERS enhancement was significantly influenced by the morphology and composition of the tetrapods. The observations in Raman spectra measurements are depicted in Figure 7, representing RhB characteristic Raman shifts: the deformation vibration of the xanthene ring (620 cm^{-1}), the C-H in-plane bend vibration (1196 cm^{-1}), the C-C bridge band stretch vibration (1279 cm^{-1}) and aromatic stretch vibrations (1359 , 1531 and 1644 cm^{-1}).

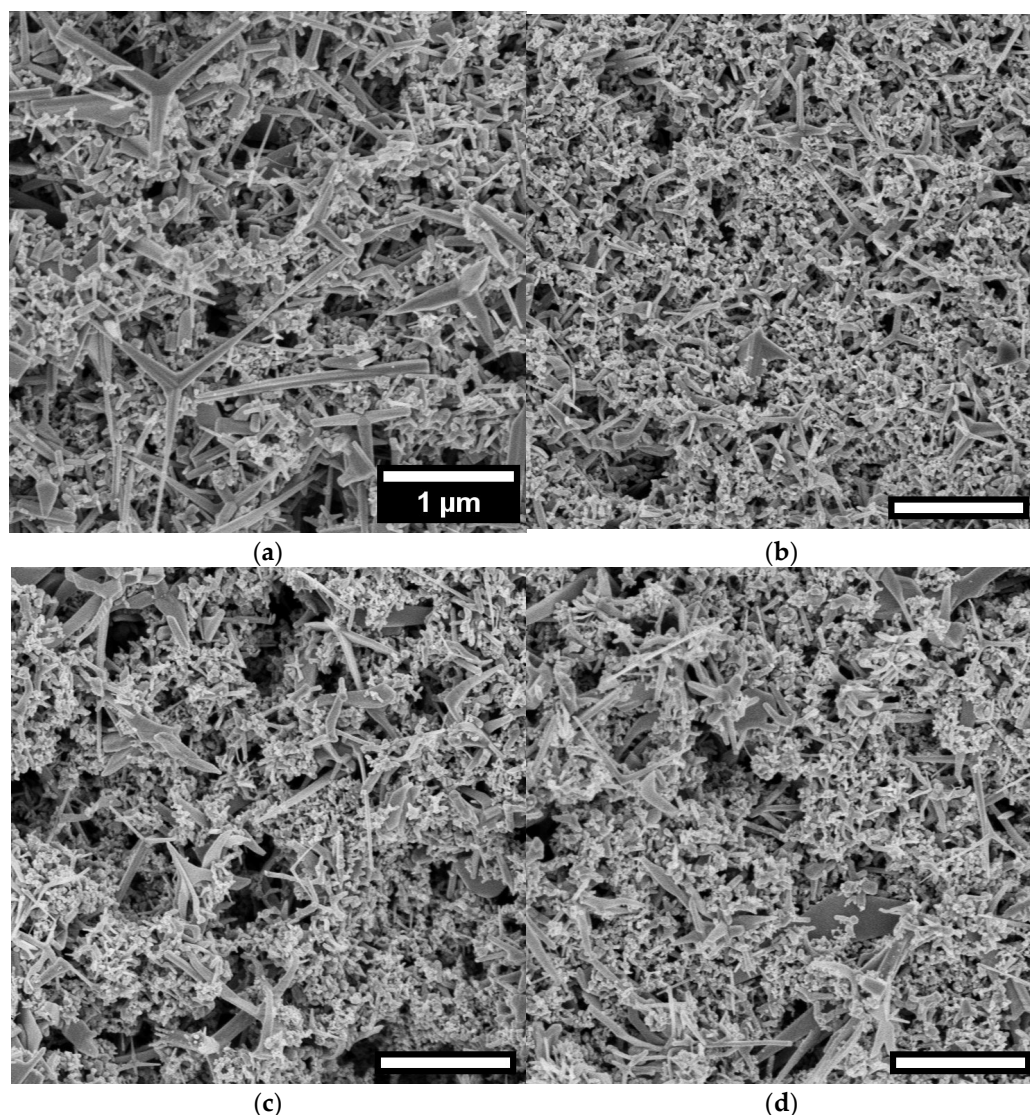


Figure 5. SEM images of ZnO-Ag tetrapod substrates synthesized from silver ion-containing zinc xerogel targets with varying silver content: (a) 0 a%; (b) 1 a%; (c) 5 a%; (d) 10 a%.

For the comparison of Raman enhancement between the substrates, the series of ZnO-Ag tetrapods obtained from silver ions containing zinc xerogel was chosen, and the most intense Raman shift at 1644 cm^{-1} was selected. The graphs of three different concentrations of RhB (6.1×10^{-5} , 6.1×10^{-6} , and 6.1×10^{-7}) are depicted in Figure 8, providing insights into the sensitivity of the SERS substrates.

Notably, the substrate synthesized from 10 atomic % silver ions containing zinc xerogel exhibited the highest Raman signal enhancement across all three concentrations of RhB. The spectra obtained from this substrate were particularly strong, indicating superior sensitivity for detecting the analyte. The significant enhancement was observable up to a concentration of 6.1×10^{-6} , highlighting the effectiveness of this substrate in amplifying Raman signals at moderate analyte concentrations. However, at the lowest concentration (6.1×10^{-7}), the Raman spectra of RhB became nearly imperceptible for all substrates, suggesting a limitation in its detection sensitivity at extremely low analyte concentrations. This observation could be attributed to factors such as the reduced interaction between the analyte and the substrate at lower concentrations. Interestingly, at the highest concentration (6.1×10^{-5}), the Raman spectra of RhB were observable for all substrates, with varying intensities. Conversely, the substrates obtained from silver nanoparticle-containing zinc dust targets showed comparatively weaker signals, suggesting differences in the SERS

enhancement capability among the substrates. The higher SERS activity for ZnO-Ag tetrapods obtained from silver ions containing zinc xerogel targets, especially 10 atomic %, most likely depends on the actual metallic silver nanoparticle content incorporated in the substrates, which is validated by the obtained results of EDX analysis.

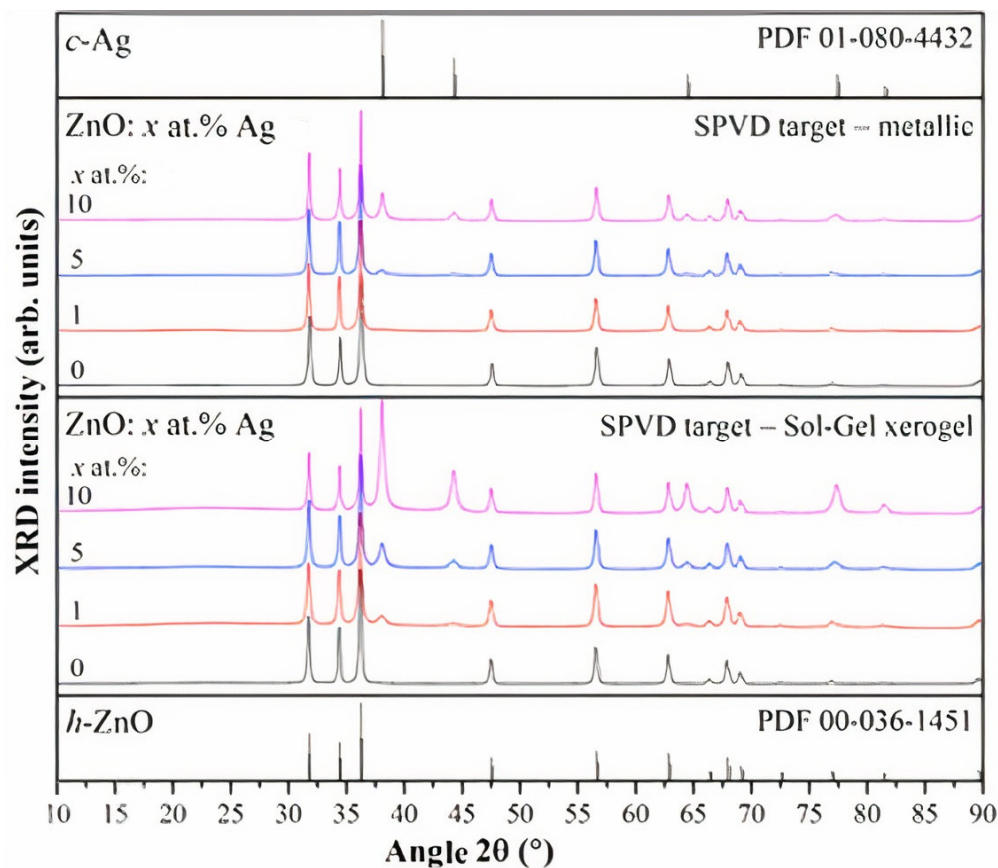
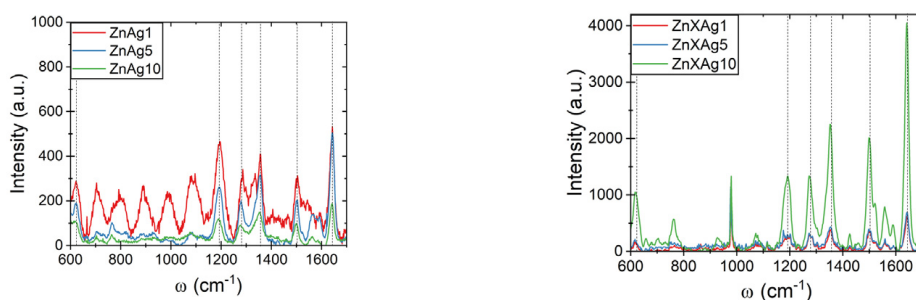


Figure 6. The obtained XRD patterns of synthesized ZnO-Ag tetrapods.



(a) RhB concentration 6.1×10^{-5} M

(b) RhB concentration. 6.1×10^{-5} M

Figure 7. Raman spectra of RhB obtained on the following: **(a)** ZnO-Ag tetrapod substrates synthesized from metallic zinc dust and metallic silver nanoparticles; **(b)** ZnO-Ag tetrapod substrates synthesized from silver ions containing zinc xerogel.

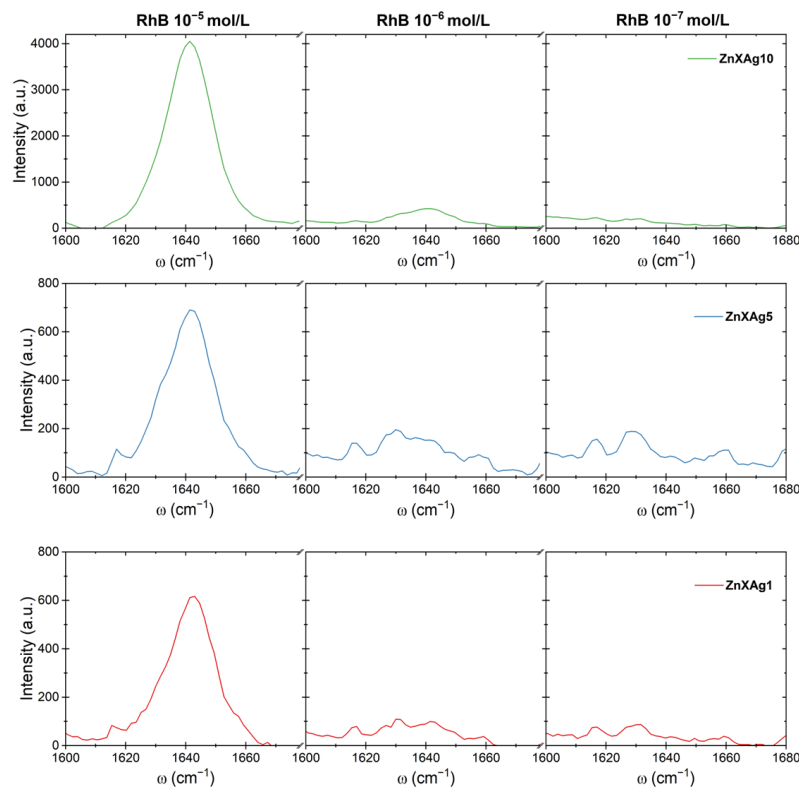


Figure 8. Raman signal enhancement of RhB on ZnO-Ag tetrapod substrates obtained from silver ion-containing zinc xerogel targets, with emphasis on the Raman shift at 1644 cm^{-1} .

4. Conclusions

There is an urgent demand for a dependable and efficient SERS substrate that is capable of amplifying signals from diverse samples to introduce SERS as a valuable tool for biochemical analysis. This study introduces an approach that addresses this need by utilizing a 3D framework composed of ZnO-Ag tetrapods. This method allows the creation of a SERS-active substrate with a high number of “hot spots”, avoiding the requirement for exceedingly tight gaps between noble metal nanoparticles, which could otherwise restrict the size of the molecules amenable to SERS analysis. Through this strategy, we formulated and refined a simple procedure for producing a SERS substrate that leverages the benefits of densely distributed, highly SERS-active nanoparticles within a three-dimensional structure, thus enhancing signal amplification. The resulting SERS substrate material demonstrates signal-enhancing properties up to $3\text{ }\mu\text{g/mL}$ for the detection of RhB. This substrate has the potential to be effective in detecting a wide array of molecules relevant to biomedical applications, including pharmaceutical compounds and viral proteins.

Author Contributions: Conceptualization, E.V. and K.S.; methodology, E.V. and I.B.; investigation, E.V., I.B., K.V. and C.F.T.; data curation, E.V., L.I. and R.I.; writing—original draft preparation, E.V.; writing—review and editing, K.S., R.I. and A.T.; visualization, K.V., L.I. and A.T.; supervision, K.S. All authors have read and agreed to the published version of the manuscript.

Funding: This research was funded by European Regional Development Fund project Nr. 1.1.1.1/21/A/053 realized at the Institute of Solid State Physics, University of Latvia.

Data Availability Statement: The supporting data will not be publicly available.

Acknowledgments: The Institute of Solid State Physics, University of Latvia, as the Center of Excellence, received funding from the European Union’s Horizon 2020 Framework Programme H2020-WIDESPREAD-01-2016-2017-TeamingPhase2 under grant agreement No. 739508, project CAMART2.

Conflicts of Interest: The authors declare no conflicts of interest.

References

1. Lin, S.; Cheng, Z.; Li, Q.; Wang, R.; Yu, F. Toward Sensitive and Reliable Surface-Enhanced Raman Scattering Imaging: From Rational Design to Biomedical Applications. *ACS Sens.* **2021**, *6*, 3912–3932. [[CrossRef](#)]
2. Szymborski, T.; Stepanenko, Y.; Niciński, K.; Piecyk, P.; Berus, S.M.; Adamczyk-Popławska, M.; Kamińska, A. Ultrasensitive SERS Platform Made via Femtosecond Laser Micromachining for Biomedical Applications. *J. Mater. Res. Technol.* **2021**, *12*, 1496–1507. [[CrossRef](#)]
3. Sitjar, J.; Liao, J.-D.; Lee, H.; Tsai, H.-P.; Wang, J.-R.; Liu, P.-Y. Challenges of SERS Technology as a Non-Nucleic Acid or -Antigen Detection Method for SARS-CoV-2 Virus and Its Variants. *Biosens. Bioelectron.* **2021**, *181*, 113153. [[CrossRef](#)]
4. Laghrib, F.; Saqrane, S.; El Bouabi, Y.; Farahi, A.; Bakasse, M.; Lahrich, S.; El Mhammedi, M.A. Current Progress on COVID-19 Related to Biosensing Technologies: New Opportunity for Detection and Monitoring of Viruses. *Microchem. J.* **2021**, *160*, 105606. [[CrossRef](#)] [[PubMed](#)]
5. Martín, J.; Tena, N.; Asuero, A.G. Current State of Diagnostic, Screening and Surveillance Testing Methods for COVID-19 from an Analytical Chemistry Point of View. *Microchem. J.* **2021**, *167*, 106305. [[CrossRef](#)] [[PubMed](#)]
6. Cui, F.; Zhou, H.S. Diagnostic Methods and Potential Portable Biosensors for Coronavirus Disease 2019. *Biosens. Bioelectron.* **2020**, *165*, 112349. [[CrossRef](#)]
7. Asif, M.; Ajmal, M.; Ashraf, G.; Muhammad, N.; Aziz, A.; Iftikhar, T.; Wang, J.; Liu, H. The Role of Biosensors in Coronavirus Disease-2019 Outbreak. *Curr. Opin. Electrochem.* **2020**, *23*, 174–184. [[CrossRef](#)] [[PubMed](#)]
8. Song, C.; Guo, S.; Jin, S.; Chen, L.; Jung, Y. Biomarkers Determination Based on Surface-Enhanced Raman Scattering. *Chemosensors* **2020**, *8*, 118. [[CrossRef](#)]
9. Maddali, H.; Miles, C.E.; Kohn, J.; O'Carroll, D.M. Optical Biosensors for Virus Detection: Prospects for SARS-CoV-2/COVID-19. *ChemBioChem* **2020**, *22*, 1176–1189. [[CrossRef](#)] [[PubMed](#)]
10. Ambrosch-Draxl, C.; Auer, H.; Kouba, R.; Sherman, E.Y.; Knoll, P.; Mayer, M. Raman Scattering in $\text{YBa}_2\text{Cu}_3\text{O}_7$: A Comprehensive Theoretical Study in Comparison with Experiments. *Phys. Rev. B* **2002**, *65*, 064501. [[CrossRef](#)]
11. Gillet, Y.; Giantomassi, M.; Gonze, X. First-Principles Study of Excitonic Effects in Raman Intensities. *Phys. Rev. B* **2013**, *88*, 094305. [[CrossRef](#)]
12. Mosier-Boss, P. Review of SERS Substrates for Chemical Sensing. *Nanomaterials* **2017**, *7*, 142. [[CrossRef](#)] [[PubMed](#)]
13. Sharma, B.; Frontiera, R.R.; Henry, A.-I.; Ringe, E.; Van Duyne, R.P. SERS: Materials, Applications, and the Future. *Mater. Today* **2012**, *15*, 16–25. [[CrossRef](#)]
14. Ali, A.; Nettey-Opong, E.E.; Effah, E.; Yu, C.Y.; Muhammad, R.; Soomro, T.A.; Byun, K.M.; Choi, S.H. Miniaturized Raman Instruments for SERS-Based Point-of-Care Testing on Respiratory Viruses. *Biosensors* **2022**, *12*, 590. [[CrossRef](#)] [[PubMed](#)]
15. Wang, X.; Zhang, E.; Shi, H.; Tao, Y.; Ren, X. Semiconductor-Based Surface Enhanced Raman Scattering (SERS): From Active Materials to Performance Improvement. *Analyst* **2022**, *147*, 1257–1272. [[CrossRef](#)] [[PubMed](#)]
16. Gaur, R.; Manikandan, P.; Manikandan, D.; Umopathy, S.; Padhy, H.M.; Maaza, M.; Elayaperumal, M. Noble Metal Ion Embedded Nanocomposite Glass Materials for Optical Functionality of UV-Visible Surface Plasmon Resonance (SPR) Surface-Enhanced Raman Scattering (SERS) X-ray and Electron Microscopic Studies: An Overview. *Plasmonics* **2021**, *16*, 1461–1493. [[CrossRef](#)]
17. Le Ru, E.C.; Meyer, M.; Blackie, E.; Etchegoin, P.G. Advanced Aspects of Electromagnetic SERS Enhancement Factors at a Hot Spot. *J. Raman Spectrosc.* **2008**, *39*, 1127–1134. [[CrossRef](#)]
18. Kim, J.; Jang, Y.; Kim, N.-J.; Kim, H.; Yi, G.-C.; Shin, Y.; Kim, M.H.; Yoon, S. Study of Chemical Enhancement Mechanism in Non-Plasmonic Surface Enhanced Raman Spectroscopy (SERS). *Front. Chem.* **2019**, *7*, 582. [[CrossRef](#)]
19. Trivedi, D.J.; Barrow, B.; Schatz, G.C. Understanding the Chemical Contribution to the Enhancement Mechanism in SERS: Connection with Hammett Parameters. *J. Chem. Phys.* **2020**, *153*, 124706. [[CrossRef](#)]
20. Mohaghegh, F.; Tehrani, A.M.; Materny, A. Investigation of the Importance of the Electronic Enhancement Mechanism for Surface-Enhanced Raman Scattering (SERS). *J. Phys. Chem. C* **2021**, *125*, 5158–5166. [[CrossRef](#)]
21. Tan, L.; Wei, M.; Shang, L.; Yang, Y. Cucurbiturils-Mediated Noble Metal Nanoparticles for Applications in Sensing, SERS, Theranostics, and Catalysis. *Adv. Funct. Mater.* **2020**, *31*, 202007277. [[CrossRef](#)]
22. Trausa, A.; Tipaldi, C.F.; Ignatane, L.; Polyakov, B.; Oras, S.; Butanovs, E.; Vanags, E.; Smits, K. Heat-Induced Fragmentation and Adhesive Behaviour of Gold Nanowires for Surface-Enhanced Raman Scattering Substrates. *Chem. Eng.* **2024**, *8*, 15. [[CrossRef](#)]
23. Samriti; Rajput, V.; Gupta, R.K.; Prakash, J. Engineering Metal Oxide Semiconductor Nanostructures for Enhanced Charge Transfer: Fundamentals and Emerging SERS Applications. *J. Mater. Chem. C* **2022**, *10*, 73–95. [[CrossRef](#)]
24. Liang, X.; Li, N.; Zhang, R.; Yin, P.; Zhang, C.; Yang, N.; Liang, K.; Kong, B. Carbon-Based SERS Biosensor: From Substrate Design to Sensing and Bioapplication. *NPG Asia Mater.* **2021**, *13*, 8. [[CrossRef](#)]
25. Li, D.; Wu, A.; Wan, Q.; Li, Z. Controllable Fabrication of Polymeric Nanowires by NIL Technique and Self-Assembled AAO Template for SERS Application. *Sci. Rep.* **2021**, *11*, 14929. [[CrossRef](#)]
26. Liu, Y.; Zhang, Y.; Tardivel, M.; Lequeux, M.; Chen, X.; Liu, W.; Huang, J.; Tian, H.; Liu, Q.; Huang, G.; et al. Evaluation of the Reliability of Six Commercial SERS Substrates. *Plasmonics* **2019**, *15*, 743–752. [[CrossRef](#)]
27. Das, G.; Mecarini, F.; Gentile, F.; De Angelis, F.; Mohan Kumar, H.; Candeloro, P.; Liberale, C.; Cuda, G.; Di Fabrizio, E. Nano-Patterned SERS Substrate: Application for Protein Analysis vs. Temperature. *Biosens. Bioelectron.* **2009**, *24*, 1693–1699. [[CrossRef](#)] [[PubMed](#)]

28. Li, J.; Yan, H.; Tan, X.; Lu, Z.; Han, H. Cauliflower-Inspired 3D SERS Substrate for Multiple Mycotoxins Detection. *Anal. Chem.* **2019**, *91*, 3885–3892. [[CrossRef](#)] [[PubMed](#)]
29. Fu, B.-B.; Tian, X.-D.; Song, J.-J.; Wen, B.-Y.; Zhang, Y.-J.; Fang, P.-P.; Li, J.-F. Self-Calibration 3D Hybrid SERS Substrate and Its Application in Quantitative Analysis. *Anal. Chem.* **2022**, *94*, 9578–9585. [[CrossRef](#)]
30. Xu, L.; Wang, Y.-Y.; Huang, J.; Chen, C.-Y.; Wang, Z.-X.; Xie, H. Silver Nanoparticles: Synthesis, Medical Applications and Biosafety. *Theranostics* **2020**, *10*, 8996–9031. [[CrossRef](#)]
31. Riswana Barveen, N.; Wang, T.-J.; Chang, Y.-H. In-Situ Deposition of Silver Nanoparticles on Silver Nanoflowers for Ultrasensitive and Simultaneous SERS Detection of Organic Pollutants. *Microchem. J.* **2020**, *159*, 105520. [[CrossRef](#)]
32. Zhang, C.; Chen, S.; Jiang, Z.; Shi, Z.; Wang, J.; Du, L. Highly Sensitive and Reproducible SERS Substrates Based on Ordered Micropyramid Array and Silver Nanoparticles. *ACS Appl. Mater. Interfaces* **2021**, *13*, 29222–29229. [[CrossRef](#)]
33. Amendola, V.; Bakr, O.M.; Stellacci, F. A Study of the Surface Plasmon Resonance of Silver Nanoparticles by the Discrete Dipole Approximation Method: Effect of Shape, Size, Structure, and Assembly. *Plasmonics* **2010**, *5*, 85–97. [[CrossRef](#)]
34. Picciolini, S.; Castagnetti, N.; Vanna, R.; Mehn, D.; Bedoni, M.; Gramatica, F.; Villani, M.; Calestani, D.; Pavesi, M.; Lazzarini, L.; et al. Branched Gold Nanoparticles on ZnO 3D Architecture as Biomedical SERS Sensors. *RSC Adv.* **2015**, *5*, 93644–93651. [[CrossRef](#)]
35. Xu, J.; Li, C.; Si, H.; Zhao, X.; Wang, L.; Jiang, S.; Wei, D.; Yu, J.; Xiu, X.; Zhang, C. 3D SERS Substrate Based on Au-Ag Bi-Metal Nanoparticles/MoS₂ Hybrid with Pyramid Structure. *Opt. Express* **2018**, *26*, 21546. [[CrossRef](#)] [[PubMed](#)]
36. Pahlow, S.; Mayerhöfer, T.; van der Loh, M.; Hübner, U.; Dellith, J.; Weber, K.; Popp, J. Interference-Enhanced Raman Spectroscopy as a Promising Tool for the Detection of Biomolecules on Raman-Compatible Surfaces. *Anal. Chem.* **2018**, *90*, 9025–9032. [[CrossRef](#)] [[PubMed](#)]
37. Mishra, Y.K.; Adelung, R. ZnO Tetrapod Materials for Functional Applications. *Mater. Today* **2018**, *21*, 631–651. [[CrossRef](#)]
38. Schindelin, J.; Arganda-Carreras, I.; Frise, E.; Kaynig, V.; Longair, M.; Pietzsch, T.; Preibisch, S.; Rueden, C.; Saalfeld, S.; Schmid, B.; et al. Fiji: An Open-Source Platform for Biological-Image Analysis. *Nat. Methods* **2012**, *9*, 676–682. [[CrossRef](#)] [[PubMed](#)]

Disclaimer/Publisher’s Note: The statements, opinions and data contained in all publications are solely those of the individual author(s) and contributor(s) and not of MDPI and/or the editor(s). MDPI and/or the editor(s) disclaim responsibility for any injury to people or property resulting from any ideas, methods, instructions or products referred to in the content.